

# MINIJETS IN ULTRARELATIVISTIC HEAVY ION COLLISIONS AT RHIC AND LHC

K.J.Eskola<sup>1</sup>

*CERN/TH, CH-1211 Geneve 23, Switzerland*

## Abstract

Recent results on minijet production in nuclear collisions at the RHIC and LHC energies are reviewed. Initial conditions of the QGP at  $\tau = 0.1$  fm/ $c$ , especially parton chemistry, thermalization and net baryon number-to-entropy ratio are discussed. Also, contribution of minijets from a hard BFKL-pomeron ladder will be estimated.

## 1 Introduction

Particle and transverse energy production in the central rapidity region of heavy ion collisions can be treated as a combination of hard/semihard parton production and soft particle production. With increasing energies, the semihard QCD-processes are expected to become increasingly important. This is due to two reasons: firstly, already in  $p\bar{p}(p)$  collisions the rapid rise of the total and inelastic cross sections can be explained by copious production of semihard partons, *minijets*, with transverse momenta  $p_T \geq p_0 \sim 1...2$  GeV [1]. This is also expected to happen in  $AA$  collisions at very high energies. Secondly, the semihard particle production scales as  $A^{4/3}$ , so that for large nuclei the importance of semihard partons is increased further [2, 3, 4]. The soft, non-perturbative, particle production in ultrarelativistic heavy ion collisions can be modelled *e.g.* through strings [5, 6, 7] or through a decaying strong background colour field [8].

The time scale for producing partons and transverse energy into the central rapidity region by semihard collisions is short, typically  $\tau_h \sim 1/p_0 \sim 0.1$  fm/ $c$ , where  $p_0 \sim 2$  GeV is the smallest transverse momentum included in the computation. The soft processes are completed at later stages of the collision, at  $\tau_s \sim 1/\Lambda_{\text{QCD}} \sim 1$  fm/ $c$ . If the density of partons produced in the hard and semihard stages of the heavy ion collision becomes high enough - as will be the case - a saturation in the initial parton production can occur [2, 9, 10, 11], and softer particle production will be screened. The fortunate consequence of this is that a larger part of parton production in the central rapidities can be *computed* from perturbative QCD (pQCD) at higher energies and the relative contribution from soft collisions with  $p_T \lesssim 2$  GeV becomes smaller. Typically, the expectation is that at the SPS (Pb+Pb at  $\sqrt{s} = 17$  AGeV), the soft component dominates, and at the LHC (Pb+Pb at  $\sqrt{s} = 5.5$  ATeV) the semihard component is the dominant one. At the RHIC (Au+Au at  $\sqrt{s} = 200$  AGeV) one will be in the intermediate region, and both components should be taken into account.

A lot of effort has also been devoted for building event generators [7, 12] addressing the dominance of semihard processes in nuclear collisions at high energies. These have generated also new insight and very useful discussion during the recent years. Also recently, a promising novel approach to minijet production has been developed [13].

---

<sup>1</sup>On leave of absence from: *Laboratory of High Energy Physics, Department of Physics, P.O.Box 9, 00014 University of Helsinki, Finland*

I have divided this talk basically into two halves. In the first one, I will recapitulate the basic features of semihard parton production and review our latest results [4, 10, 11]. The main goal of these studies is to find out the initial conditions for early QGP-formation at  $\tau \sim 0.1$  fm/c, including the transverse energy deposited into the mid-rapidity region, chemical composition of the parton plasma, and, to study the possibility of a very rapid thermalization and estimate the initial net baryon-to-entropy ratio. It is vitally important to study the early formation of strongly interacting partonic matter, since the later evolution of the QGP, the final state global observables, and the suggested signals of the plasma will strongly depend on the initial conditions. The second half I will devote for discussion of an additional mechanism for parton and transverse energy production: minijets from a BFKL-ladder [14]. Especially, I will estimate the maximum amount of transverse energy one should expect from the BFKL-minijets in heavy ion collisions.

## 2 Initial conditions for QGP at $\tau \sim 0.1$ fm/c

Hadronic jets originating from high  $p_T$  quarks and gluons are clearly observed experimentally but when the partons have  $p_T \lesssim 5$  GeV the jets become very difficult to distinguish [15] from the underlying event. In heavy ion collisions, where we expect hundreds (RHIC) or thousands (LHC) of minijets with  $p_T \sim 2$  GeV be produced, detection of individual minijets will be impossible. However, the semihard partons are expected to contribute dramatically to the early formation of QGP. The idea of multiple production of semihard gluons and quarks in  $pp$  and  $AA$  collisions is based on a picture of independent binary parton-parton collisions. The key quantity is the integrated jet cross section,

$$\sigma_{\text{jet}}(\sqrt{s}, p_0) = \frac{1}{2} \int_{p_0^2} dp_T^2 dy_1 dy_2 \sum_{\substack{ijkl= \\ q, \bar{q}, g}} \int dy_2 x_1 f_{i/N}(x_1, Q) x_2 f_{j/N}(x_2, Q) \frac{d\hat{\sigma}^{ij \rightarrow kl}}{d\hat{t}}(\hat{s}, \hat{t}, \hat{u}), \quad (1)$$

where  $x_{1,2}$  are the fractional momenta of the incoming partons  $i$  and  $j$ , and  $f_{i/N}(x, Q)$  are the parton distributions in  $N$  ( $= p, A$ ). The factor 2 comes from the fact that, in the lowest order (LO) pQCD, there are two partons produced in each semihard subcollision. In the eikonal models for  $pp$  collisions [1] the ratio  $\sigma_{\text{jet}}/\sigma_{\text{inelastic}}$  can be interpreted as the average number of semihard events in one inelastic collision. The results I will be quoting in the following [4] are obtained with the MRSH [16] and MRSD-' [17] parton distributions with a scale choice  $Q = p_T$ . More detailed formulation can be found in Refs. [3, 11], and numerical evaluation of Eq. (1) in Ref. [4].

The formula above is defined in the lowest order (LO),  $d\hat{\sigma}/d\hat{t} \sim \alpha_s^2$ . Often a constant factor  $K \sim 2$  is used to simulate the effects of NLO terms. Studies of the NLO jet cross section  $d\sigma/(dp_T dy)$  [19] show that (with a scale choice  $Q = p_T$  and with a jet size  $R \sim 1$ ) this is a reasonable approximation [18]. Strictly speaking, however, a theoretical  $K$ -factor can only be defined for quantities where a well-defined, infrared-safe measurement function can be applied [19]. For  $E_T$ -production in nuclear collisions, an acceptance window in the whole central rapidity unit defines such a function but for this acceptance criteria and for  $p_T \sim 2$  GeV the exact NLO contribution has not been computed yet.

The first estimate of the average number of produced semihard partons with  $p_T \geq p_0$  in an  $AA$  collision at a fixed impact parameter  $\mathbf{b}$  can be obtained as [3]

$$\bar{N}_{AA}(\mathbf{b}, \sqrt{s}, p_0) = 2T_{AA}(\mathbf{b})\sigma_{\text{jet}}(\sqrt{s}, p_0), \quad (2)$$

and the average transverse energy carried by these partons as [3]

$$\bar{E}_T^{AA}(\mathbf{b}, \sqrt{s}, p_0) = T_{AA}(\mathbf{b})\sigma_{\text{jet}}(\sqrt{s}, p_0)\langle E_T \rangle, \quad (3)$$

where  $T_{AA}(\mathbf{b})$  is the nuclear overlap function [3] which scales  $T_{AA} \sim A^{4/3}$ , describing thus the typical scaling of hard processes in nuclear collisions. The normalization is  $\int d^2\mathbf{b}T_{AA}(\mathbf{b}) = A^2$  and, for large nuclei with Woods-Saxon nuclear densities,  $T_{AA}(\mathbf{0}) \approx A^2/(\pi R_A^2)$ . The acceptance criteria imposed for the quantities  $\sigma_{\text{jet}}(\sqrt{s}, p_0)$  and for  $\sigma_{\text{jet}}(\sqrt{s}, p_0)\langle E_T \rangle$  will be  $|y| \leq 0.5$ , and the corresponding cuts will be made in  $y_1$  and  $y_2$ . In Eqs. (2) and (3) above,  $T_{AA}(\mathbf{b})\sigma_{\text{jet}}$  is the average number of semihard collisions and  $\langle E_T \rangle$  is the average transverse energy carried by the partons produced in each of these collisions. We fix  $p_0 = 2$  GeV, *i.e.* we describe the initial conditions at  $\tau \sim 1/p_0 = 0.1$  fm/ $c$ . The predictions for the central rapidity unit in Pb-Pb collisions at the RHIC and LHC energies are summarized in Tables 1. Also, contributions from gluon, quark and antiquark production are shown separately [4].<sup>2</sup>

In the results given, we have neglected nuclear effects in parton distributions:  $f_{i/A} = Af_{i/p}$ . In reality, however, in the typical  $x$ -region  $x \sim 2p_0/\sqrt{s}$  there are quite strong shadowing corrections [20], especially for the LHC nuclear collisions. Also, the scale evolution of nuclear gluon shadowing was shown to be potentially important in the analysis in Ref. [21]. However, a re-analysis with the input from HERA at small- $x$  [22] has to be performed before getting a solid quantitative prediction of the shadowing effects on minijet production.

The rapid rise of the structure function  $F_2(x, Q)$  at small values of  $x$  observed at HERA [22] does not affect the bulk of the 2 GeV minijets at RHIC energies very much but obviously has quite dramatic consequences at the LHC energies. As demonstrated in [4], there is a clear enhancement of minijet production due to the new parton distributions. However, the more rapidly the gluon distributions rise, the more there should be nuclear shadowing due to the GLRMQ-fusions [9, 23, 24]. Again, a more quantitative prediction depends on the scale evolution of nuclear gluon shadowing as well.

Let us now have a closer look at the results in Table 1. There are four important observations. Firstly, the gluons clearly dominate both the initial parton and transverse energy production: the initial parton system is about 80 % glue.

Secondly, the effective transverse area of the produced semihard partons is  $\bar{N}_{AA}\pi/p_0^2$ . Comparing this with the effective nuclear transverse area,  $\pi R_A^2$ , we notice that

$$\xi_A \equiv \frac{\bar{N}_{AA}\pi/p_0^2}{\pi R_A^2} \sim 1 \text{ for LHC} \quad \text{and} \quad \xi_A \ll 1 \text{ for RHIC}, \quad (4)$$

*i.e.* the parton system at the LHC at 0.1 fm/ $c$  is already dense enough so that a saturation of parton production can take place [2, 9, 11]. In this way, the scale  $p_0$  acquires also *dynamical* significance. At RHIC, since  $\xi_A < 1$ , saturation occurs at smaller values of  $p_T$  (at  $\tau > 0.1$  fm/ $c$ ), possibly in the region where pQCD cannot be trusted. This qualitative argumentation

---

<sup>2</sup>Results for  $d\sigma/(dp_T dy)$  at  $y = 0$  can be found in Ref. [10].

| $\bar{N}_{\text{PbPb}}$ | total | $g$  | $q$  | $\bar{q}$ |
|-------------------------|-------|------|------|-----------|
| LHC:                    | 3252  | 2710 | 276  | 266       |
|                         | 5978  | 5220 | 385  | 373       |
| RHIC:                   | 200   | 156  | 26.3 | 17.4      |
|                         | 199   | 157  | 25.7 | 16.6      |

| $E_{\text{T}}^{\text{PbPb}}$ | total | $g$   | $q$  | $\bar{q}$ |
|------------------------------|-------|-------|------|-----------|
| LHC                          | 10310 | 8640  | 854  | 816       |
|                              | 17580 | 15330 | 1150 | 1100      |
| RHIC                         | 547   | 426   | 73.6 | 47.0      |
|                              | 539   | 422   | 71.7 | 44.8      |

Table 1: **(a)** The average numbers of semihard partons at  $\tau = 0.1$  fm/c with  $|y| \leq 0.5$  and  $p_{\text{T}} \geq 2$  GeV in central Pb-Pb collisions, as given by Eq. (2). Shadowing is not included and  $K = 2$ . The upper values are obtained with MRSH and the lower ones with MRSD-' parton distributions. **(b)** The average transverse energy carried by these partons, as predicted by Eq. (3).

is supported by a more quantitative, although still phenomenological, analysis of Ref. [10], where we suggested that at sufficiently large energies (LHC) and large nuclei ( $A \sim 200$ ), a dynamical screening mass is generated, causing a saturation in the minijet cross sections [10] at a perturbative scale like  $p_0 \sim 2$  GeV  $\gg \Lambda_{\text{QCD}}$ . The consequence is that the softer parton production is screened and its relative importance becomes smaller.<sup>3</sup>

The third interesting observation is that the gluonic subsystem in the central rapidity unit  $\Delta y = 1$  may thermalize very fast, at least in the LHC nuclear collisions. In the perturbatively produced system the (transverse) energy per gluon is  $\bar{E}_{\text{T}}^g / \bar{N}_{\text{PbPb}}^g = \epsilon_g^{\text{pQCD}} / n_g^{\text{pQCD}} \approx 3$  GeV and the energy density of the system at  $\tau_{\text{h}} = 0.1$  fm/c is  $\epsilon_g^{\text{pQCD}} = \bar{E}_{\text{T}}^g / (\pi R_A^2 \tau_{\text{h}} \Delta y)$ . The temperature  $T_{\text{eq}}$  of an ideal (massless boson) gas in a complete thermal (= both kinetic and chemical) equilibrium with this energy density can be computed from  $\epsilon_g^{\text{ideal}} = 3\pi^2 / 90 \cdot 16 T_{\text{eq}}^4 = \epsilon_g^{\text{pQCD}}$ , and we get  $T_{\text{eq}} = 0.988$  (1.14) GeV with the MRSH (MRSD-') densities. Especially, we find [4]

$$\frac{\epsilon_g^{\text{pQCD}}}{n_g^{\text{pQCD}}} \sim \frac{\epsilon_g^{\text{ideal}}}{n_g^{\text{ideal}}} \text{ for LHC} \quad \text{and} \quad \frac{\epsilon_g^{\text{pQCD}}}{n_g^{\text{pQCD}}} > \frac{\epsilon_g^{\text{ideal}}}{n_g^{\text{ideal}}} \text{ for RHIC}, \quad (5)$$

so that at the LHC the average energy of gluons is already as in an ideal gas in thermal equilibrium. Only isotropization is needed, and a rapid thermalization is indeed possible. An instant thermalization would in turn have profound consequences on *e.g.* thermal dileptons, for which a high initial temperature plays a crucial role [25].<sup>4</sup>

Note that our conclusion of the possibility of an almost instant thermalization is due to the small- $x$  enhancement in the HERA gluon densities. From the energy/gluon viewpoint it also seems that thermalization for RHIC is going to happen somewhat later. Note however, that above I did not consider isotropization of the system at all. In the simplified picture presented here, the transit time of the colliding nuclei,  $\tau_{\text{tr}} \sim 2R_A/\gamma$ , and the initial parton spread,  $\Delta z \sim 1/(xp) \sim 1/p_0$  for the partons which will be produced in the mid-rapidity, are neglected. Then a Bjorken-like boost-invariant picture is possible, and in the central rapidities a proper time  $\tau$  is a relevant variable. For a more thorough discussion of isotropization, a more detailed microscopic space-time picture has to be specified, as done in Refs. [12, 26] (see also the discussion in [11, 10]).

<sup>3</sup>A similar saturation effect is also expected in the approach by McLerran *et al.* [13].

<sup>4</sup>On the other hand, for the thermal dileptons the trouble is the small out-of-equilibrium quark-antiquark component of the early parton system.

The fourth observation [11] is that initially, at  $\tau \sim 0.1$  fm/ $c$ , the net baryon number density in the central rapidity unit is very small as compared to the gluon density but *larger* than the nuclear matter density ( $0.17$  fm $^{-3}$ ), even though the colliding nuclei are practically already far apart, especially at the LHC where  $\tau_{\text{tr}} \ll \tau_{\text{h}}$ . More precisely, we estimate

$$n_{B-\bar{B}} \equiv \frac{1}{3}(n_q - n_{\bar{q}}) = \frac{\frac{1}{3}(\bar{N}_q - \bar{N}_{\bar{q}})}{\pi R_A^2 \Delta y / p_0} = \begin{cases} 0.25 (0.30) \text{ fm}^{-3}, & \text{for LHC} \\ 0.22 (0.23) \text{ fm}^{-3}, & \text{for RHIC} \end{cases} \quad (6)$$

with the MRSH (MRSD-') parton distributions. Computing the net baryon-to-entropy ratio by using  $s_g = 3.6n_g$  for a thermal boson gas gives *initially*, at  $\tau = 0.1$  fm/ $c$ :  $(B - \bar{B})/S_g \sim 2 \cdot 10^{-4}$  for LHC, and  $\sim 2 \cdot 10^{-3}$  for RHIC. We conclude that at the future colliders we are still relatively far away from the extreme conditions of the Early Universe, where the inverse of the specific entropy is  $\sim 10^{-9}$  [27]. For the LHC, assuming an instant thermalization of the gluon system at  $\tau = 0.1$  fm/ $c$ , and an adiabatic evolution thereafter, the final entropy can be approximated by the initial entropy of gluons [4, 11]. The non-perturbative mechanism for particle production will not increase the entropy much but does increase the net baryon number. If the non-perturbative contribution to the net baryon number production is assumed to be of the same order of magnitude as in the current Pb+Pb collisions at SPS, the *final* baryon-to-entropy ratio for the LHC will be  $\sim 10^{-3}$ . For the RHIC nuclear collisions, thermalization is most likely not as instantaneous, but following nevertheless the same line of arguments, and taking into account that the non-perturbative component becomes important also for entropy production, we estimate  $\sim 10^{-2}$  for the final net baryon-to-entropy ratio.

### 3 Minijets in the BFKL-approach

Minijet production I have considered above is based on collinear factorization, where the perturbative partonic cross sections are factorized at a momentum scale  $Q \sim p_{\text{T}}$  from the parton distributions with nonperturbative input. Next, I will discuss an additional mechanism for minijet and transverse energy production, where factorization is not used.

The small- $x$  rise in the structure function  $F_2(x, Q^2)$  observed at HERA  $Q^2 > 1.5$  GeV $^2$  [22] can be explained by the leading  $\log(Q^2)$  DGLAP-evolution [28] and also by the leading  $\log(Q^2) \log(1/x)$  evolution [29]. Also a power-like behaviour,  $F_2 \sim x^{-\delta}$ , expected in the leading  $\log(1/x)$  BFKL-approach [30], does not contradict the data. In the following, let us assume that the small- $x$  increase is entirely due to the BFKL-physics. Then, with this assumption, we will study what is the *maximum* transverse energy deposit in the central rapidity unit due to the minijets emitted from a BFKL-ladder in the LHC nuclear collisions. At RHIC the BFKL-minijets are not expected to contribute in any significant manner because the BFKL-enhancement takes place only at  $x \lesssim 0.01$ . Therefore, this latter part of my talk, which is based on Ref. [14], will be relevant only for the LHC.

It is instructive to start from a case of fully inclusive minijets with two tagging jets separated by a wide rapidity gap, as studied by Mueller and Navelet [31]. The (summed) subprocess is also shown Fig. 1a, where the incoming partons have momentum fractions  $x_a$  and  $x_b$ , the tagging jets rapidities  $y_a$  and  $y_b$  ( $y_a \gg y_b$ ) and transverse momenta  $\mathbf{k}_{a\text{T}}$  and  $\mathbf{k}_{b\text{T}}$ , respectively. Between the tagging jets there are  $n$  gluons emitted, labeled by  $1 \dots n$ . Thus

each final state is described by a Feynman graph with 2 incoming and  $n + 2$  outgoing on-shell gluons. The colour singlet hard BFKL-pomeron ladder arises when these Feynman graphs are squared and summed. In the kinematic region we will be interested in, the rapidities are strongly ordered,  $y_a \gg y_1 \gg \dots \gg y_n \gg y_b$ , but the transverse momenta are not,  $\mathbf{k}_{Ti} \sim \mathbf{k}_{Tj}$ . Then only the transverse degrees of freedom of the momenta of the virtual legs become important. The tagging jets of Fig. 1a have transverse momenta at a perturbative scale, so that one may use collinear factorization to write the cross section down as:

$$\frac{d\sigma}{d^2\mathbf{k}_{aT}d^2\mathbf{k}_{bT}dy_ady_b} = \sum_{n=0}^{\infty} x_a g(x_a, \mu^2) x_b g(x_b, \mu^2) \int \prod_{i=1}^n \frac{dy_i}{4\pi} \frac{d^2\mathbf{k}_{iT}}{(2\pi)^2} \frac{|M_{a1\dots nb}|^2}{16\pi^2 \hat{s}^2} \delta^{(2)}\left(\sum_{j=0}^{n+1} \mathbf{k}_{jT}\right), \quad (7)$$

where only gluons are considered. The strong rapidity ordering simplifies the momentum fractions to  $x_a \approx \frac{k_{aT}}{\sqrt{s}} e^{y_a}$  and  $x_b \approx \frac{k_{bT}}{\sqrt{s}} e^{-y_b}$ , and the parton densities factor out of the sum.

For the process  $gg \rightarrow gg$  the leading contribution in the large  $\hat{s}/\hat{t}$  limit comes from the  $t$ -channel amplitude. In a physical gauge, this amplitude is also gauge invariant up to the subleading terms. The matrix element  $M_{a1\dots nb}$  consists then of the following building blocks: In the leading  $\hat{s}/\hat{t}$  approximation, in a physical gauge and with the strong rapidity ordering, each gluon can be regarded as emitted from an effective non-local Lipatov-vertex, where bremsstrahlung from initial and final legs and emission from the exchanged gluon are summed. These are described by the black blobs in Fig 1. Also the propagators are effective ones since they are exponentiated (Reggeized) after computing the leading virtual corrections to the  $t$ -channel gluon exchange. The effective propagators are drawn by thicker (vertical) lines in Fig. 1. Original references, detailed discussion and derivation of these concepts can be found in the useful lecture notes by Del Duca [32].

Next, we square each matrix element  $M_{a1\dots nb}$ , and due to the strong ordering in rapidities, colour singlet ladders with  $n + 2$  rungs are formed. The colour algebra can be performed by summing (averaging) over the final (initial) state colours, and the polarization sums can be done. With help of *e.g.* Laplace-transformation (in  $y_a - y_b$ ), the rapidity integrals can be disentangled. Finally, by summing over  $n$ , one obtains an iterative integral equation, the inhomogeneous BFKL-equation [30, 31] (see also [32]), which describes an addition of one rung into the colour-singlet hard pomeron ladder. The BFKL-ladder is denoted by  $f(\mathbf{q}_T, \mathbf{k}_T, y_a - y_b)$  in Fig 1a. The cross section (7) then becomes:

$$\frac{d\sigma}{d^2\mathbf{k}_{aT}d^2\mathbf{k}_{bT}dy_ady_b} = x_a g(x_a, \mu^2) x_b g(x_b, \mu^2) \frac{4N_c^2 \alpha_s^2}{N_c^2 - 1} \frac{1}{k_{aT}^2} 2f(\mathbf{q}_T, \mathbf{k}_T, y_a - y_b) \frac{1}{k_{bT}^2}, \quad (8)$$

where  $\mathbf{q}_T = -\mathbf{k}_{aT}$  and  $\mathbf{k}_T = \mathbf{k}_{bT}$ . If all the virtual corrections and the real emissions are neglected, the ladder reduces into  $2f(\mathbf{q}_T, \mathbf{k}_T, y) \rightarrow \delta^{(2)}(\mathbf{q}_T - \mathbf{k}_T)$ , and the Born limit for the two jets separated by a large rapidity interval is recovered [32].

Let us then study the case with tagging jets further by fixing one step of the ladder, as shown in Fig. 1b. It is straightforward to sum the graphs with gluon emissions between the tagging jet  $a$  and the fixed minijet  $c$ , and, between the minijet  $c$  and the tagging jet  $b$ . This creates a ladder on each side of the fixed rung. Especially, we learn that a generic factor  $\alpha_s N_c / (\pi^2 k_{cT}^2)$ , which includes the phase-space factor and contraction of the two Lipatov vertices associated with the step  $c$ , arises from fixing the the rung  $c$ . The cross section

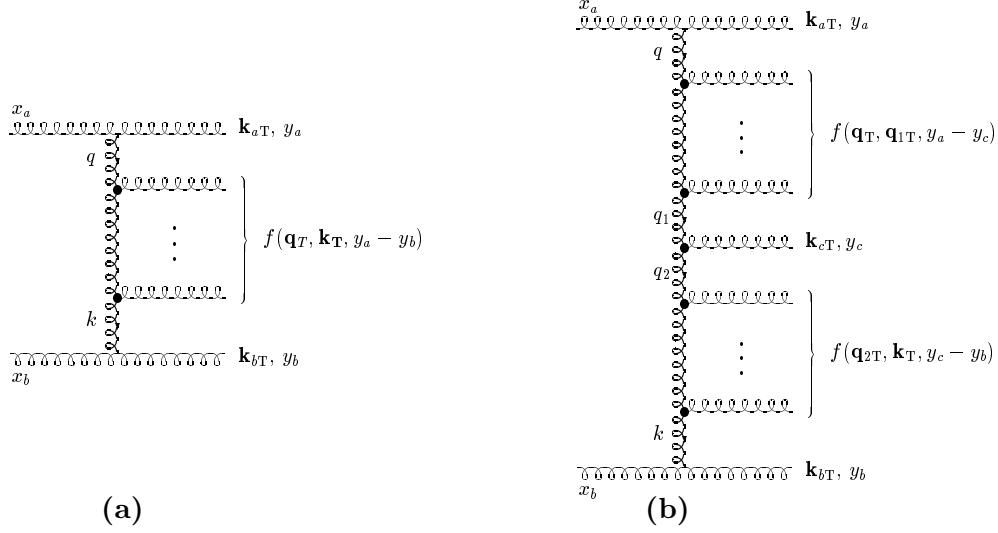


Figure 1: (a) The BFKL ladder in fully inclusive minijet production between the two tagging jets  $a$  and  $b$  [31, 9, 33]. (b) Fixing one step of the ladder (c) creates a ladder on each side of the minijet  $c$  [34].

becomes [34]

$$\frac{d\sigma}{d^2\mathbf{k}_{aT}d^2\mathbf{k}_{bT}d^2\mathbf{k}_{cT}dy_a dy_b dy_c} = x_a g(x_a, \mu^2) x_b g(x_b, \mu^2) \frac{4N_c^2 \alpha_s^2}{N_c^2 - 1} \frac{\alpha_s N_c}{\pi^2} \frac{1}{k_{cT}^2} \int d^2\mathbf{q}_{1T} d^2\mathbf{q}_{2T} \cdot \delta^{(2)}(\mathbf{k}_{cT} - \mathbf{q}_{1T} + \mathbf{q}_{2T}) \frac{2f(\mathbf{k}_{aT}, \mathbf{q}_{1T}, y_a - y_c)}{k_{aT}^2} \frac{2f(\mathbf{q}_{2T}, \mathbf{k}_{bT}, y_c - y_b)}{k_{bT}^2}. \quad (9)$$

Our goal is to study the leading BFKL minijet production mechanism which is  $\sim \alpha_s$ . As illustrated in Fig. 2, we therefore relax the requirement of having tagging jets. Then coupling of the pomeron ladder to the hadron becomes essentially non-perturbative and a form-factor, or, rather, a parton distribution, will be needed. Also, now that we do not require any tagging jets, we have to give up collinear factorization. We do not have any perturbative Born limit to compare with, either. Therefore, the best we can do is to adopt the procedure for deep inelastic scattering (DIS) in [35], where an addition of each rung into the pomeron ladder between the two hadrons or nuclei is expected to be described by the *homogeneous* BFKL equation for the unintegrated gluon density  $f(x, q_T^2)$ ,

$$-x \frac{\partial f(x, q_T^2)}{\partial x} = \frac{\alpha_s N_c}{\pi} q_T^2 \int_0^\infty \frac{dq_{1T}^2}{q_{1T}^2} \left[ \frac{f(x, q_{1T}^2) - f(x, q_T^2)}{|q_T^2 - q_{1T}^2|} + \frac{f(x, q_T^2)}{\sqrt{q_T^4 + 4q_{1T}^4}} \right]. \quad (10)$$

Normalization for this scale-invariant equation is given by the gluon distributions

$$xg(x, Q^2) = \int^{Q^2} \frac{dq_T^2}{q_T^2} f(x, q_T^2), \quad (11)$$

determined from experimental input [35].

By using the knowledge of the factor arising from fixing one rung of the BFKL-pomeron ladder, the inclusive minijet cross section from the BFKL-ladder can now be written down

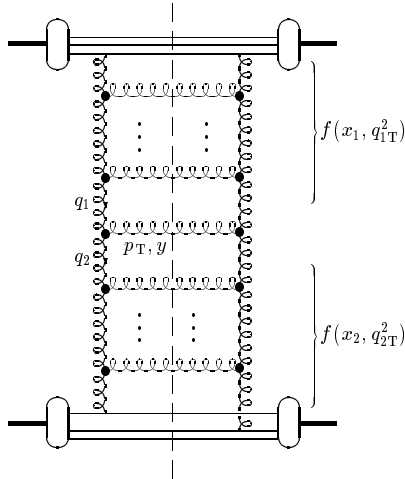


Figure 2: Minijet production without the tagging jets requires an introduction of unintegrated parton distributions  $f(x, q_T^2)$  [33].

as [33, 14]

$$\frac{d\sigma^{\text{jet}}}{d^2\mathbf{p}_T dy} = K_N \frac{\alpha_s N_c}{\pi^2} \frac{1}{p_T^2} \int d^2\mathbf{q}_{1T} d^2\mathbf{q}_{2T} \delta^{(2)}(\mathbf{p}_T - \mathbf{q}_{1T} + \mathbf{q}_{2T}) \frac{f(x_1, q_1^2)}{q_{1T}^2} \frac{f(x_2, q_2^2)}{q_{2T}^2} \quad (12)$$

where  $p_T$  and  $y$  are the transverse momentum and the rapidity (in the hadron CMS) of the minijet. From momentum conservation and multi-Regge kinematics the momentum fractions become  $x_{1(2)} \approx \frac{p_T}{\sqrt{s}} e^{\pm y}$ . Due to the fact that in this case we do not have an “external” hard probe like the virtual photon with an associated quark box as in DIS, nor an on-shell Born cross section to relax into, we cannot determine the overall dimensionless normalization constant  $K_N$  exactly. However, we are able to fix the *slope* of the minijet  $p_T$ -distribution, which will be sufficient for estimating the upper limit of transverse energy production from the BFKL-ladder.

The minijet cross section of Eq. (12) is shown in Fig. 3 [14]. In the BFKL-computation we have used the unintegrated gluon densities compatible with the small- $x$  rise in the set MRS-D’ [17]. For comparison, the more traditional (CFLTLO) minijet cross sections, discussed in the first half of the talk, are also shown with the MRSD-’ parton distributions. The NLO jet analysis [19, 18] indicates that LO+NLO calculation with collinear factorization reproduces the measured jet cross sections well. Therefore, at  $p_T \gtrsim 5$  GeV, the BFKL-minijet contribution should be less than the collinearly factorized. We can thus argue that  $K_N \lesssim 1$ .

The transverse energy production due to the minijets from the BFKL-ladders at  $|y| \leq 0.5$  in  $AA$  collisions can now be estimated [14] from

$$\left. \frac{d\bar{E}_T^{\text{BFKL}}}{dy} \right|_{y=0} = T_{AA}(\mathbf{b}) \int_{p_0^{\text{BFKL}}} dp_T p_T \left. \frac{d\sigma^{\text{jet}}}{dp_T dy} \right|_{y=0}. \quad (13)$$

The coherence of the BFKL ladder is broken when we fix a rung, and the cross section diverges at  $p_T \rightarrow 0$ . A cut-off is, unfortunately, needed also in the BFKL case. The saturation of the CFLTLO-minijet cross section in the LHC Pb-Pb collisions (as considered in the first half of the talk), implies that the BFKL-cross section should not grow much larger than



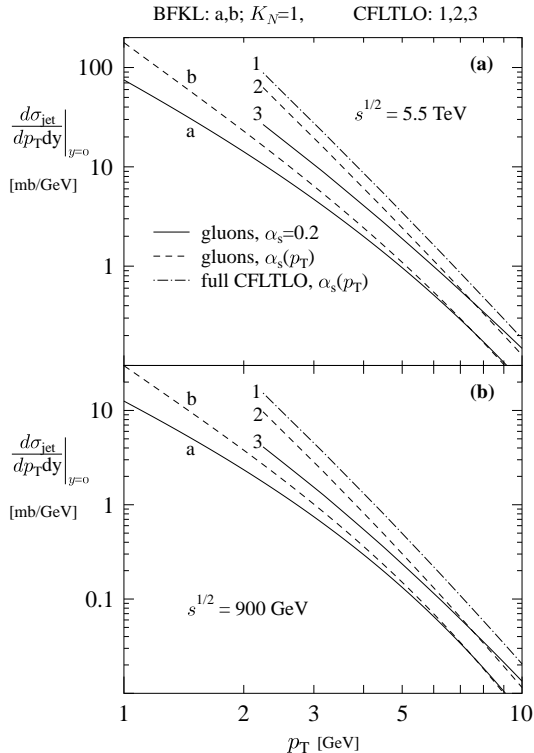


Figure 3: The minijet cross sections at  $y = 0$  as functions of transverse momentum  $p_T$  at  $\sqrt{s} = 5.5$  TeV from [14]. (panel a) and  $\sqrt{s} = 900$  GeV (panel b) [14]. The curves 1, 2 and 3 are predicted in the approach of collinear factorization, leading twist and lowest order (CFLTLO) pQCD, and MRSD-' parton distributions. The curves a and b are the BFKL-minijets from Eq. (12) with and without running coupling.

the curve 2 in Fig. 3. Therefore, we do not trust the BFKL-computation with  $K_N \sim 1$  below  $p_T \leq p_0^{\text{BFKL}} \sim 1$  GeV. With these values, we find for central Pb-Pb collisions at the LHC,  $\bar{E}_T^{\text{BFKL}} = 3060$  GeV with fixed  $\alpha_s = 0.2$ , and, 4940 GeV with (*ad hoc*) running  $\alpha_s(p_T)$ . Comparing these numbers to the value 15330 GeV in Table 1b for gluons, we see that the BFKL-contribution is at most a few 10% correction to the results in [4, 11]. On the other hand, one should perhaps compare the results at the same level of approximations, (only LO gluons,  $\alpha_s$  fixed) *i.e.* curves 3 and a in Fig. 3a. Then the two contributions become of similar magnitude. In this case, however, the  $p_0$  in the CFLTLO-computation should be lower than 2 GeV, and the BFKL contribution would again be the smaller one.

We worked under the assumption that the BFKL-evolution is responsible for *all* the small- $x$  rise at HERA, *i.e.* we studied the *maximum* contribution from the kinematical region relevant for the hard BFKL-pomeron. Since the HERA results can be explained by the leading  $\log(Q^2)$  and/or the leading  $\log(Q^2) \log(1/x)$  approximations, the leading  $\log(1/x)$ -contribution is obviously not the dominant mechanism at the present values of  $x$ . Thus, my conclusion is that the BFKL-minijets certainly bridge the way towards softer physics at  $p_T < p_0 \sim 2$  GeV, but the initial conditions relevant for the early QGP-formation in the LHC nuclear collisions are dominantly given by the minijets computed in collinear factorization.

**Acknowledgements.** The results discussed in this talk are based on Refs. [4, 10, 11, 14]. I would like to thank K. Kajantie, A. Leonidov, B. Müller, V. Ruuskanen and X.-N. Wang

for fruitful collaboration. I also owe special thanks to A. Leonidov and V. Ruuskanen for getting our BFKL-study started and finally finished.

## References

- [1] X.-N. Wang, Phys. Rev. **D43** (1991) 104, and references therein.
- [2] J.-P. Blaizot and A. Mueller, Nucl. Phys. **B289** (1987) 847.
- [3] K. Kajantie, P. V. Landshoff and J. Lindfors, Phys. Rev. Lett. **59** (1987) 2517; K.J. Eskola, K. Kajantie and J. Lindfors, Nucl. Phys. **B323** (1989) 37.
- [4] K.J. Eskola, K. Kajantie and V. Ruuskanen, Phys. Lett. **B332** (1994) 191.
- [5] B. Andersson, G. Gustafson, B. Nilsson-Almqvist, Nucl. Phys. **B281** (1986) 289.
- [6] K. Werner, Phys. Rep. 232 (1993) 87.
- [7] X.-N. Wang and M. Gyulassy, Phys. Rev. **D44** (1991) 3501; *ibid.* **D45**, 844 (1992) 844; Phys. Rev. Lett. **68** (1992) 1480; Comput. Phys. Commun. **83** (1994) 307.
- [8] K. Kajantie and T. Matsui, Phys. Lett. **B164**(1985) 373; G. Gattoff, A. K. Kerman and T. Matsui, Phys. Rev. **D36** (1987) 114; K.J. Eskola and M. Gyulassy, Phys. Rev. **C47** (1993) 2329.
- [9] L. V. Gribov, E. M. Levin and M. G. Ryskin, Phys. Rep. **100** (1983) 1.
- [10] K.J. Eskola, B. Müller and X.-N. Wang, Phys. Lett. B374 (1996) 20; B. Müller, in this workshop.
- [11] K.J. Eskola and K. Kajantie, Preprint CERN-TH/96-259, September 1996.
- [12] K. Geiger and B. Müller, Nucl. Phys. **B369** (1992) 600; K. Geiger, Phys. Rev. **D47** (1993) 133.
- [13] A. Kovner, L. Mc Lerran and H. Weigert, Phys. Rev. **D52** (1995) 3809, 6231; R. Venugopalan, Preprint DOE/ER/ 40561-251-INT96-00-120, March 1996.
- [14] K.J. Eskola, A. Leonidov and P.V. Ruuskanen, Preprint CERN-TH/96-124.
- [15] UA1 Collaboration, C. Albajar *et al.*, Nucl. Phys. **B309** (1988) 405.
- [16] A.D. Martin, W.J. Stirling and R.G. Roberts, RAL preprint 93-077 (1993).
- [17] A.D. Martin, W.J. Stirling and R.G. Roberts, Phys. Lett. **B306** (1993) 145.
- [18] K.J. Eskola and X.-N. Wang, Int. J. Mod. Phys. **A10** (1995) 2881.
- [19] S.D. Ellis, Z. Kunszt and D.E. Soper, Phys. Rev. Lett. **69** (1992) 1496; Z. Kunszt and D. E. Soper, Phys. Rev. **D46** (1992) 192.
- [20] NM Collaboration, P. Amaudruz *et al.*, Z. Phys. **C51** (1991) 387.
- [21] K.J. Eskola, Nucl. Phys. **B400** (1993) 240.
- [22] H1 Collaboration, I. Abt *et al.*, Nucl. Phys. **B407** (1993) 515; T. Ahmed *et al.*, Nucl. Phys. **B439** (1995) 471; ZEUS Collaboration, M. Derrick *et al.*, Phys. Lett. **B316** (1993) 412; Z. Phys. **C65** (1995) 379.
- [23] A. Mueller and J. Qiu, Nucl. Phys. **B268** (1986) 427.
- [24] E.M. Levin, in this workshop.
- [25] P.V. Ruuskanen, Proc. *Quark Matter 91*, Nucl. Phys. **A544** (1992) 169c.
- [26] K.J. Eskola and X.-N. Wang, Phys. Rev. **D49** (1994) 1284; T.S. Biró, E. van Doorn, B. Müller, M.H. Thoma and X.-N. Wang, Phys. Rev. **C48** (1993) 1275.
- [27] U. Heinz, “Heavy ion physics at the LHC”, in Proc. of *Towards the LHC Experimental Programme*, ECFA meeting, 5-8 March 1992, Evian-les-Bains, France, p. 95.
- [28] Yu. Dokshitzer, Sov. Phys. JETP **46** (1977) 1649; V. N. Gribov and L. N. Lipatov, Sov. Nucl. Phys. **15** (1972) 438, 675; G. Altarelli, G. Parisi, Nucl. Phys. **B126** (1977) 298.
- [29] R. D. Ball and S. Forte, Phys. Lett. **B351** (1995) 313; *ibid* **B359** (1995) 362; *ibid* **B336** (1994) 77.
- [30] E. A. Kuraev, L. N. Lipatov and V. S. Fadin, Sov. Phys. JETP **45** (1977) 199; Ya. Ya. Balitskij and L. N. Lipatov, Sov. J. Nucl. Phys. **28** (1978) 822.
- [31] A. H. Mueller and H. Navelet, Nucl. Phys **B282** (1987) 727.
- [32] V. Del Duca, “An introduction to the perturbative QCD pomeron and to jet physics at large rapidities”, DESY 95-023, February 1995.
- [33] L. V. Gribov, E. M. Levin and M. G. Ryskin, Phys Lett. **B100** (1981) 173; Phys Lett. **B121** (1983) 65; E. M. Levin and M. G. Ryskin, Phys. Rep. **189** (1990) 267.
- [34] V. Del Duca, M. E. Peskin and W.-K. Tang, Phys. Lett. **B306** (1993) 151.
- [35] A. J. Askew, J. Kwieciński, A. D. Martin and P. J. Sutton, Phys. Rev. **D49** (1994) 4402.